Lattice QCD in strong magnetic fields

P.V.Buividovich[ab], *M.N.Chernodub*[cdb §], *E.V.Luschevskaya*[b], *M.I.Polikarpov*[b]
[a] *JIPNR "Sosny", National Academy of Science, Krasin str. 99, Minsk, Belarus*
[b] *ITEP, B. Cheremushkinskaya 25, Moscow, 117218 Russia*
[c] *CNRS, LMPT, Fédération Denis Poisson, Université de Tours, 37200 France*
[d] *DMPA, University of Gent, Krijgslaan 281, S9, B-9000 Gent, Belgium*

Abstract

Vacuum of Quantum Chromodynamics in very strong (hadron-scale) magnetic fields exhibits many interesting nonperturbative effects. Some of these effects can be studied with the help of lattice simulations in quenched QCD. We review our recent results demonstrating that very strong external magnetic fields lead to (1) the enhancement of the chiral symmetry breaking [the quark condensate rises with the increase of the external magnetic field]; (2) the chiral magnetization of the QCD vacuum [spins of the quarks turn parallel to the external field]; (3) the chiral magnetic effect [a CP-odd generation of the electric current of quarks directed along the magnetic field]; (4) a CP-odd generation of the anomalous quark electric dipole moment along the axis of magnetic field. The first three effects were already predicted theoretically, and subsequently observed numerically in our simulations, while the fourth effect is a new result.

1 Introduction

Motivation

Noncentral heavy-ion collisions may create very strong magnetic field due to relative motion of electrically charged ions and the products of the collision. This fact ignited the interest of the scientific community towards an investigation of the properties of the strongly interacting matter exposed to the magnetic field. The QCD effects should be visible because the strength of the created magnetic field may be of the order of the hadron-scale, or higher. For example, at first moments ($\tau \sim 1\,\mathrm{fm/c}$) of Au-Au collision at the Relativistic Heavy Ion Collider (RHIC) the strength of the magnetic field may reach $eB \sim (10 - 100\,\mathrm{MeV})^2$ [1, 2]. The strong magnetic fields will also be created in the future experiments at the Facility for Antiproton and Ion Research (FAIR) at GSI, at the ALICE experiment at LHC, and at the Nuclotron-based Ion Collider fAcility (NICK) at Dubna.

§Speaker.

Vacuum effects due to strong magnetic field in QCD

There are various vacuum effects which appear due to the strong external magnetic fields (here we do not discuss interesting phenomena that may emerge in a dense quark matter).

Enhancement and shift of the chiral phase transition. Theoretically, the very strong magnetic fields may significantly modify the QCD phase diagram [3, 4]. The external magnetic field increases the transition temperature and enhances the strength of the (phase) transition from the chirally broken (low temperature) phase to the chirally restored (high temperature) phase. Moreover, in the external magnetic field the transition – which is a smooth crossover in the absence of the fields – becomes a first order transition [3, 4].

Enhancement of the chiral symmetry breaking. The magnetic field stabilizes the chirally broken (low-temperature) phase of QCD by enlarging the value of the chiral condensate and enhancing the chiral symmetry breaking. This result was obtained in various approaches using the chiral perturbation theory [5, 6, 7], the Nambu-Jona-Lasinio model [8], the linear sigma model [9] and the AdS/QCD dual description [10]. In lattice simulations this effect was observed in our recent work [11]. In Section 2 we discuss main results of [11].

Chiral magnetization. Another effect of the strong enough magnetic field is a (para)magnetic response of the QCD vacuum: the external fields polarize the spins (or, equivalently, the magnetic moments) of the quarks and antiquarks, leading to the chiral magnetization of the vacuum. At relatively low magnetic fields the chiral magnetization is proportional to the strength of the magnetic field. The coefficient of the proportionality, called the chiral magnetic susceptibility, was first discussed in Ref. [12] in order to analyze phenomenologically interesting nucleon magnetic moments. The value of the magnetic susceptibility – which was estimated using various analytical approaches [13, 14, 15, 16, 17, 18] – can be measured in experiments on lepton pair photoproduction [19], in radiative heavy meson decays [20], etc. At higher magnetic fields the behavior of the magnetization deviates from a linear function as it gets affected by logarithmic corrections at moderately strong fields [21]. At asymptotically strong fields the magnetization reaches an upper bound. The first lattice investigation of the chiral magnetization was performed in Ref. [22]. The results of [22] are briefly described in Section 3.

Chiral Magnetic Effect. The magnetic fields may lead to quite unusual effects due to the nontrivial topological structure of the QCD vacuum [1, 23]. We discuss a particular realization of the Chiral Magnetic Effect (CME), which gives rise to a generation of an *electric* current along the direction of the *magnetic* field in a nontrivial topological backgrounds of gluons [1]. The potentially observed feature of the CME is a non-statistical asymmetry in the number of positively and negatively charged particles emitted on different sides of the reaction plane in the heavy-ion collisions [24]. There are preliminary indications

that this $\mathcal{CP}$-odd effect has been indeed observed by the STAR Collaboration in experiments at RHIC [25]. In our lattice studies we found the existence of the CME both at vacuum and thermal ground states of gluon fields, and at specially prepared configurations with nontrivial topological charge [26]. The main results of Ref. [26] are given in Section 4.

Quark electric dipole moment. Another manifestation of a nontrivial topological structure of the QCD vacuum is an appearance of an *electric* dipole moment of a quark along the direction of the external *magnetic* field. This $\mathcal{CP}$-odd effect – which is a spin analogue of the Chiral Magnetic Effect – is observed in lattice simulations in Ref. [27]. The lattice evidence of the generation of the quark's electric dipole moment is discussed in Section 5.

Physical setup and technical details of simulations

We utilize lattice QCD with the simplest $SU(2)$ gauge group because all studied effects originate in the chiral sector of QCD where the number of colors is not crucial. In our simulations only valence quarks interact with the electromagnetic field, and the effects of the virtual quarks on gluons are neglected. Indeed, the inclusion of dynamical (sea) quarks makes the simulations computationally difficult, while the essential features of all mentioned effects are visible in the quenched limit as well (an extended discussion is given in [11, 22, 26, 28]).

The chiral effects are best studied with massless fermions. In order to implement chirally symmetric massless fermions on the lattice, we use Neuberger's overlap Dirac operator [29]. We reduce the ultraviolet lattice artifacts using the tadpole-improved Symanzik action for the gluons. We introduce the magnetic field $B_\mu = B\delta_{\mu 3}$ into the Dirac operator by substituting $su\,(2)$-valued vector potential A_μ with $u\,(2)$-valued field. In infinite volume such substitution is $A_\mu^{ij} \to A_\mu^{ij} + C_\mu \delta^{ij}$, where $C_\mu = B\,(x_2\delta_{\mu 1} - x_1\delta_{\mu 2})\,/2$ is the external $U(1)$ gauge field. In the finite volume L^4 with periodic boundary conditions an additional x-dependent boundary twist for the fermion fields should be introduced [30], and the uniform magnetic field is forced to take quantized values [31], $qB = 2\pi\, k/L^2$, where $k \in \mathbb{Z}$ and $q = 1/3\,|e|$ is the absolute value of the electric charge of the d-quark. Note that in all figures below we indicate the magnetic field strength in units of $qB \equiv eB/3$ and not in eB. In our simulations the *lowest* magnetic field takes values $\sqrt{eB} \sim (400 - 600\,\mathrm{MeV})^2$. Such fields are stronger than those expected at RHIC, while they are of same order as the magnetic fields that will presumably be created at the LHC collisions [2].

In order to check the finite-volume effects we use two spatial lattice volumes, 14^3 and 16^3. We study the system at three different temperatures, $T/T_c = 0,\ 0.82,\ 1.12$ (the critical temperature in $SU(2)$ gauge theory is $T_c \approx 310\,\mathrm{MeV}$). In order to make sure that the influence of the finite ultraviolet cutoff is under proper control, we utilize three lattice spacings, $a = 0.089\,\mathrm{fm},\ 0.103\,\mathrm{fm},\ 0.128\,\mathrm{fm}$. Our spatial volumes range from $L^3 = (1.4\,\mathrm{fm})^3$ to $(2\,\mathrm{fm})^3$.

2 Enhancement of chiral condensate

The chiral condensate

$$\Sigma \equiv -\langle 0|\, \bar{q}q \,|0\rangle \,, \tag{1}$$

is commonly used order parameter for the chiral symmetry breaking in the theory with massless quarks. The condensate is zero if the chiral symmetry is unbroken. If the strength of magnetic field is larger than the pion mass (which is zero for massless quarks) but is still much smaller than the hadronic scale, one can use the chiral perturbation theory to calculate the field dependence of the chiral condensate. According to the original work [5], in a leading order in B, the chiral condensate $\Sigma(B)$ rises linearly with the field strength:

$$\Sigma(B) = \Sigma(0) \left(1 + \frac{eB \ln 2}{16\pi^2 F_\pi^2}\right) , \tag{2}$$

where $F_\pi \approx 130\,\mathrm{MeV}$ is the pion decay constant. The corrections due to non-vanishing pion mass may also be calculated [7].

The condensate (1) can be calculated using the Banks-Casher formula [32],

$$\Sigma = \lim_{\lambda \to 0} \lim_{V \to \infty} \frac{\pi \rho(\lambda)}{V} \tag{3}$$

where V is the total four-volume of Euclidean space-time. The density $\rho(\lambda)$ of eigenvalues λ_n of the Dirac operator $\mathcal{D} = \gamma^\mu \left(\partial_\mu - iA_\mu\right)$ is defined by

$$\mathcal{D}\psi_n = \lambda_n \psi_n \,, \qquad \rho(\lambda) = \langle \sum_n \delta(\lambda - \lambda_n) \rangle \,, \tag{4}$$

where ψ_n are the eigenmodes of the Dirac operator.

According to Eq. (3) the enhancement of the chiral condensate in the magnetic field means that the Dirac eigenvalues in the vicinity of $\lambda = 0$ should become denser as the magnetic fields increases. In order to check this fact we plot in Figure 1 (left) the dependence of lowest Dirac eigenvalues on the strength of the magnetic field. One can clearly see that the increase of the strength of the magnetic field leads to the consolidation of the near-zero modes. This configuration has topological charge equal to one, and therefore the configuration contains one exact zero mode, $\lambda = 0$, in agreement with the Atyah-Singer theorem. The presence of the zero mode is independent of the strength of the external Abelian magnetic field because the number of zero eigenmodes is equal to the topological charge of the gauge field configuration, while the topological charge is not affected by the Abelian magnetic field.

In Figure 1 (right) we show the chiral condensate as the function of the magnetic field qB at zero temperature and at $T = 0.82\,T_c$. Following (2) we fit the chiral condensate by the linear function,

$$\Sigma(B) = \Sigma_0 \left(1 + \frac{eB}{\Lambda_B^2}\right) , \tag{5}$$

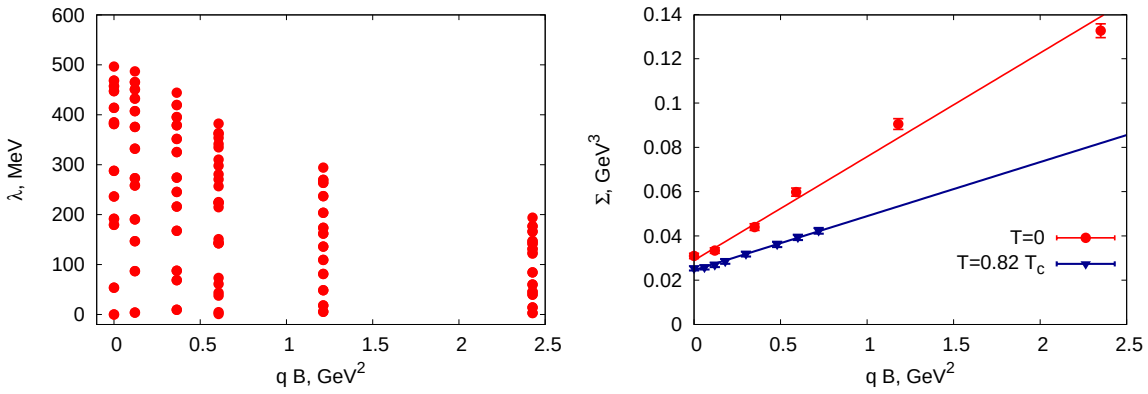

Figure 1: (left) The spectrum of lowest twelve eigenvalues λ (including the zero mode $\lambda = 0$) of the Dirac operator in a background of a typical gluon configuration vs the magnetic field qB. (right) The chiral condensate vs qB at two different temperatures T. The solid lines are the linear fits by the function (5). Figures are from [11].

where Σ_0 and Λ_B are the fitting parameters.

The best fits are shown in Figure 1 (right) by the solid lines. The best fit parameters at zero and nonzero temperatures are, respectively [11]:

$$T = 0: \qquad \Sigma_0^{\rm fit} = [(320 \pm 5)\ {\rm MeV}]^3, \qquad \Lambda_B^{\rm fit} = (1.53 \pm 0.11)\ {\rm GeV}, \quad (6)$$

$$T = 0.82\, T_c: \qquad \Sigma_0^{\rm fit} = [(291 \pm 1)\ {\rm MeV}]^3, \qquad \Lambda_B^{\rm fit} = (1.74 \pm 0.03)\ {\rm GeV}. \quad (7)$$

We see that the increase of temperature leads to a decrease the chiral condensate (as expected), and to a decrease the slope of the B-dependence.

The zero-field zero-temperature best fit value (6) of the chiral condensate, $\Sigma_0^{\rm fit}$, agrees very well with other numerical estimations in quenched $SU(2)$ gauge theory [33]. Surprisingly, the numerical value of the slope parameter Λ_B is quite close to the $T = 0$ result of the chiral perturbation theory (2), Ref. [5]:

$$\Lambda_B^{\rm theory} = 4\pi F_\pi/\sqrt{\ln 2} = 1.97\,{\rm GeV}\,. \quad (8)$$

The similarity between the theoretical prediction (8) and first principle $T = 0$ result (6) should be taken with care. First, we are studying the quenched theory, in which the virtual charged pions are absent, and what we observe is the effect of the gauge fields. Second, the strength of our weakest magnetic fields is still greater than the scale imposed by the zero-field chiral condensate, $\Sigma_0^{1/3}$. In this regime the prediction (2) of Ref. [5] should not work, in general, as the linear behavior is expected to be realized for much weaker fields. Thus, the observed linear enhancement of the chiral condensate in the absence of the pion loops is an intriguing unexpected feature of the non-Abelian gauge theory exposed to very intense external magnetic fields.

3 Magnetization of QCD vacuum

Quarks are spin-1/2 particles carrying magnetic moments. The magnetic moments are polarized by the external magnetic field. A natural quantitative measure of the polarization is given by the expectation value[1] [12]

$$\langle\overline{\Psi}\Sigma_{\alpha\beta}\Psi\rangle = \chi(F)\,\langle\overline{\Psi}\Psi\rangle\,qF_{\alpha\beta}\,, \tag{9}$$

where $\Sigma_{\alpha\beta} = \frac{1}{2i}[\gamma_\alpha\gamma_\beta - \gamma_\beta\gamma_\alpha]$ is the relativistic spin operator, $F_{\mu\nu} = \partial_\mu a_\nu - \partial_\nu a_\mu$ is the strength tensor of the electromagnetic field a_μ.

The right hand side of Eq. (9) is proportional to the electromagnetic field strength tensor due to the Lorenz covariance. The proportionality to the chiral condensate $\langle\overline{\Psi}\Psi\rangle$ (evaluated at the nonzero external electromagnetic field F) allows us to disentangle nonlinear effects of the enhancement of the chiral condensate in the external magnetic field (discussed in the previous Section) from the effects of the quark's spin polarization. The strength of the vacuum polarization is characterized by the chiral magnetic susceptibility $\chi(F)$.

The (chiral) magnetization of the QCD vacuum in the external magnetic field $B = F_{12} = -F_{21}$ can be described by the dimensionless quantity

$$\mu(qB) = \chi(qB)\,qB \qquad \Longleftrightarrow \qquad \langle\overline{\Psi}\Sigma_{12}\Psi\rangle = \mu(qB)\langle\overline{\Psi}\Psi\rangle\,. \tag{10}$$

In [22] we derived a magnetization analogue of the Banks-Casher formula (3):

$$\langle\overline{\Psi}\Sigma_{\alpha\beta}\Psi\rangle = \lim_{\lambda\to 0}\Big\langle \frac{\pi\nu(\lambda)}{V}\int d^4x\,\psi^\dagger_\lambda(x)\,\Sigma_{\alpha\beta}\,\psi_\lambda(x)\Big\rangle\,. \tag{11}$$

Moreover, we have proven theoretically in [22] and also checked numerically, that the following factorization rule holds:

$$\langle\overline{\Psi}\,\Sigma_{\alpha\beta}\,\Psi\rangle = \langle\overline{\Psi}\Psi\rangle\Big\langle\int d^4x\,\psi^\dagger_\lambda(x)\,\Sigma_{\alpha\beta}\,\psi_\lambda(x)\Big\rangle\,. \tag{12}$$

The comparison of this formula with Eqs. (9) and (10) gives

$$\mu(qB) \equiv \chi(qF)\,qF_{\alpha\beta} = \lim_{\lambda\to 0}\Big\langle\int d^4x\,\psi^\dagger_\lambda(x;B)\,\Sigma_{12}\,\psi_\lambda(x;B)\Big\rangle\,, \tag{13}$$

where $\psi_\lambda(x;F)$ is the eigenmode of the Dirac operator in the external (magnetic) background field $B = F_{12}$.

We established the factorization property (12) for all studied values of the magnetic fields. The comparison of the left and right sides of Eq. (12) evaluated at the same set of configurations is shown in Figure 2 (left). While both estimations agree with each other within error bars, the factorized definition (13) is much more accurate compared to the nonfactorized one (11).

[1] Flavor and spinor indices are omitted in (9). Below we consider one quark flavor for simplicity.

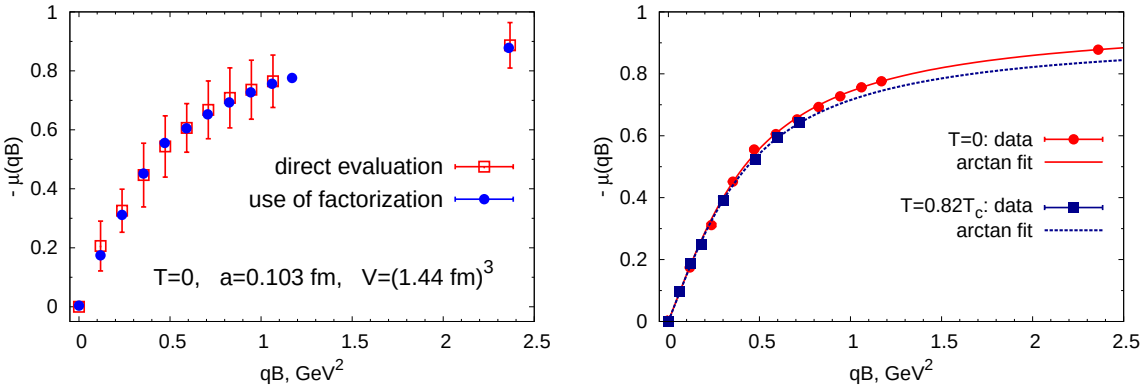

Figure 2: The magnetization μ vs the magnetic field qB. (left) Check of the factorization (12): the empty squares and the full circles show the nonfactorized (11) and factorized (13) definitions, respectively. (right) The magnetization μ at two temperatures. The lines correspond to the best fits (14). Figures are from Ref. [22].

We show in Figure 2 (right) the magnetization for two different temperatures, $T = 0$ and $T = 0.82\,T_c$. The behavior of the magnetization is consistent with general expectations: at low magnetic fields the magnetization is a linear function, which indicates the existence of a nonzero susceptibility at vanishingly small external magnetic field. At high magnetic fields the quarks are fully polarized and the magnetization approaches the saturation regime, $\mu(qB) \to -1$.

We fit our data by the function (other fitting functions are discussed in [22])

$$\mu^{\rm trig}_{\rm fit}(B) \;=\; \frac{2\mu_\infty}{\pi}\arctan\frac{\pi\chi_0 qB}{2\mu_\infty}\,, \qquad (14)$$

which has two fitting parameters: the zero-field susceptibility χ_0 and the infinite-field saturation parameter μ_∞. The fits – shown by the lines in Figure 2 (right) – give the following values for the chiral susceptibility:

$$\chi_0 = \begin{cases} -1.547(6)\;\;{\rm GeV}^{-2} & \Lambda_{\rm UV}\sim 2\,{\rm GeV} & T=0 \\ -1.53(3)\;\;{\rm GeV}^{-2} & \Lambda_{\rm UV}\sim 1.5\,{\rm GeV} & T=0.82T_c \end{cases} \qquad (15)$$

where T is the temperature, and $\Lambda_{\rm UV}$ is the momentum scale, at which the susceptibility is evaluated (the momentum dependence is discussed, e.g., in [14]).

An experimentally relevant and phenomenologically interesting quantity is the product $\chi\langle\overline{\Psi}\Psi\rangle$ at vanishing field [19]. Our data give the following result:

$$\chi\,\langle\overline{\Psi}\Psi\rangle = -46(3)\,{\rm MeV} \qquad [\text{quenched limit}]\,. \qquad (16)$$

which is surprisingly close to the estimation based on the QCD sum rules techniques, $\chi\,\langle\overline{\Psi}\Psi\rangle \approx -50\,{\rm MeV}$ [13].

4 Chiral Magnetic Effect

In brief, the physical mechanism behind the Chiral Magnetic Effect (CME) is as follows [1]. A strong magnetic field forces the magnetic moment of quarks to turn parallel to the direction of the field. If the quarks are light (massless) then the left-handed quarks will move, say, towards the direction of the magnetic field while the right-handed quarks will move backwards. If there is an imbalance between left-handed and right-handed quarks, then a net electric current $j_\mu(x) = \overline{\psi}(x)\gamma_\mu\psi(x)$ appears along the magnetic field [1, 23, 34]. This longitudinal electric current may lead also to a spatial separation of the electric charges. The longitudinal current and the spatial charge separation are the consequences of the CME. The chiral imbalance may be created by topologically nontrivial configurations of gluon fields. Generally, the CME is a reflection of the $\mathcal{CP}$-odd structure of the vacuum. The existence of the CME was demonstrated in lattice simulations in Ref. [26].

In Figure 3 we plot a spatial excess of the charge density originating due to the applied magnetic field, $j_0(x;B) = \langle j_0(x)\rangle_B - \langle j_0(x)\rangle_{B=0}$. The subtraction of the zero-field density removes all ultraviolet contributions providing us with a nonperturbative quantity. The magnetic field applied to a typical gluon configuration leads to a spatial separation of the electric charges in an agreement with the CME. The effect increases as the magnetic field gets stronger.

In Figure 4 the profile of the longitudinal (parallel to the magnetic field) and transverse (perpendicular to the field) components of the quark's electric current in a background of a specially-prepared smooth instanton-like ($Q = 1$) configuration subjected to an external magnetic field. The CME is characterized by enhancement of the longitudinal current with respect to the transverse one. This property is clearly seen in the case of the instanton, Figure 4.

Coming back to real quantum configurations of the gluonic fields, we plot in Figure 5 (left) the expectation values of the fluctuations of each component of the electric current at zero temperature. We do not distinguish the global topological charge of each configuration since the CME effect appears also locally (an extended discussion of this point is given in Ref. [26]). In agreement with the CME features, we observe the dominance of the longitudinal components of the electric current with respect to the transverse ones.

The CME crucially depends on the (local) imbalance between the left and right chiral modes given by the local chiral charge $\rho_5(x) = \overline{\psi}(x)\gamma_5\psi(x)$. The local strength of the chiral imbalance is characterized the expectation value of the chirality fluctuations, $\langle\rho_5^2\rangle$, which is shown in Figure 5 (right) for three different temperatures. At $T = 0$ the fluctuations quickly grow with the increase of the magnetic field. As the temperature increases the growth rate gets smaller, and in the deconfinement phase the rate is almost zero. In the confinement phase ($T = 0$) the chirality fluctuations at strong enough magnetic fields are as large as the fluctuations in the deconfinement phase. This fact allows us to suggest that the CME may be observed in a cold nuclear matter as well.

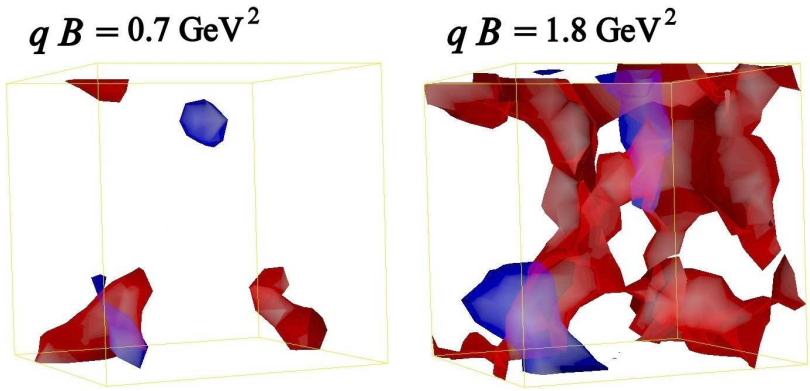

Figure 3: A visual evidence of the CME at a typical $T = 0$ gluon configuration: the excess of the positive (red) and negative (blue) electric charge due to the magnetic field (directed vertically) $qB = 0.7\,\mathrm{GeV}^2$ (left) and $qB = 1.8\,\mathrm{GeV}^2$ (right), Ref. [26].

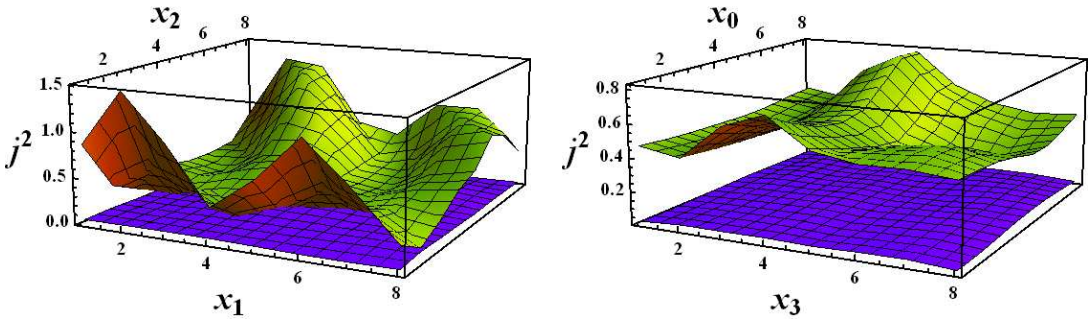

Figure 4: An evidence of the CME at an instanton-like configuration of unit topological charge: a magnetic field induces the electric current j. The upper (green) and lower (blue) surfaces are the longitudinal ($j_\parallel^2 = j_0^2 + j_3^2$) and the transverse ($j_\perp^2 = j_1^2 + j_2^2$) currents in the 12-plane (left) and in the 30-plane (right), Ref. [26].

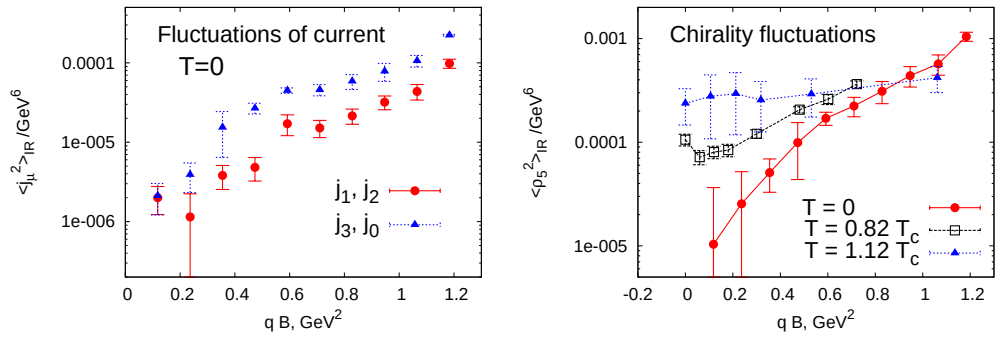

Figure 5: (left) The squares of the transverse (j_1, j_2) and longitudinal (j_3, j_0) components of the current vs the magnetic field qB at $T = 0$. (right) The chirality squared vs the magnetic field qB at various temperatures T. Figures are from Ref. [26].

5 Quark electric dipole moment

The CME induces the electric dipole moment due to the spatial charge separation along the direction of the magnetic field. Another manifestation of a nontrivial topological structure of the QCD vacuum is the appearance of the *quark* electric dipole moment directed along the axis of the external magnetic field. As in the case of the CME, the bulk average of the quark electric dipole moment is zero ($\langle \overline{\Psi} \vec{\sigma}^E \Psi \rangle = 0$) due to the global CP-invariance of the QCD vacuum. However, this anomalous effect may be seen on the event-by-event basis: locally the electric dipole moment of a quark may be large, while its sign may be alternating as the quark travels trough local fluctuations of the topological charge. In order to evaluate the magnitude of the local electric dipole moment of the quark, we study the following connected expectation values:

$$\langle (\sigma_3^\ell)^2 \rangle_{IR} \;=\; \left\langle (\sigma_3^\ell - \langle \sigma_3^\ell \rangle)^2 \right\rangle_{B,T} - \left\langle (\sigma_3^\ell - \langle \sigma_3^\ell \rangle)^2 \right\rangle_{B,T=0}, \quad \ell = E,\, M\,, \tag{17}$$

where $\sigma_i^E(x) = \overline{\psi}\,(x)\,\Sigma_{i0}\psi\,(x)$ is the local density of the electric dipole moment [the density of its magnetic counterpart is $\sigma_i^M(x) = \frac{1}{2}\varepsilon_{ijk}\overline{\psi}\,(x)\,\Sigma_{jk}\psi\,(x)$].

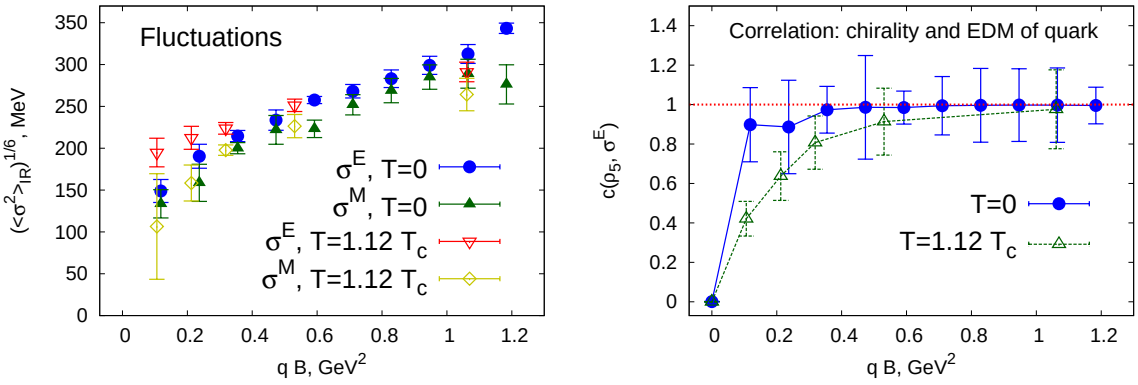

Figure 6: (left) The fluctuations of the longitudinal components the magnetic and electric dipole densities vs qB at $T = 0$ and $T = 1.12\,T_c$. (right) The correlation of the electric dipole moment of quark (EDM) with the chiral density vs qB.

In Figure 6 (left) we show values of the fluctuations of the longitudinal (i.e., directed along the magnetic field) component of the dipole moments (17). The fluctuations of the electric and magnetic dipole moments are equally strong in both phases. The transverse fluctuations of both electric and magnetic dipole moments are zero within our error bars.

The electric dipole moment of the quark is closely related to the local chirality. In Figure 6 (right) we plot the (normalized) correlator of the electric dipole moment with the chiral density, $c\left(\rho_5, \sigma_3^E\right) = \langle \rho_5\, \sigma_3^E \rangle / [\langle \rho_5^2 \rangle \langle (\sigma_3^E)^2 \rangle]^{1/2}$. At strong magnetic field we observe the very strong correlation of these two

quantities in both confinement and deconfinement phases, while at weaker magnetic fields the correlation decreases. We also observed that the thermal fluctuations suppress the correlation function $c\left(\rho_5, \sigma_3^E\right)$, and that magnetic moment is not correlated with the local chirality.

Thus, we found an evidence that the external magnetic field forces the quark to develop a local electric dipole moment along the direction of the field.

Acknowledgments

The authors are grateful to Ph. Boucaud, V.G. Bornyakov, V.V. Braguta, A.S. Gorsky, B.L. Ioffe, B.O. Kerbikov, D. Kharzeev, A. Krikun, S.M. Morozov, V.A. Novikov, B. Pire, V.I. Shevchenko, M.I. Vysotsky, and V.I. Zakharov for interesting discussions and suggestions. This work was partly supported by Grants RFBR Nos. 08-02-00661-a and 09-02-00629, grants for scientific schools Nos. NSh-679.2008.2 and Nsh-4961.2008.2, by the Russian Federal Agency for Nuclear Power, and by the STINT Institutional grant IG2004-2 025. P.V.B. is also partially supported by the Euler scholarship from DAAD, by a scholarship of the Dynasty Foundation and by the grant BRFBR F08D-005 of the Belarusian Foundation for Fundamental Research. The calculations were partially done on the MVS 50K at Moscow Joint Supercomputer Center.

References

[1] D.E. Kharzeev, L.D. McLerran, and H.J. Warringa, Nucl. Phys. A **803**, 227 (2008) [arXiv:0711.0950]; K. Fukushima, D.E. Kharzeev, and H.J. Warringa, Phys. Rev. D **78**, 074033 (2008) [arXiv:0808.3382]; H.J. Warringa, arXiv:0906.2803; D.E. Kharzeev, arXiv:0906.2808.

[2] V. Skokov, A. Illarionov and V. Toneev, arXiv:0907.1396.

[3] N. O. Agasian and S. M. Fedorov, Phys. Lett. B **663**, 445 (2008).

[4] E. S. Fraga and A. J. Mizher, Phys. Rev. D **78**, 025016 (2008) [arXiv:0804.1452]; Nucl. Phys. A **820**, 103C (2009) [arXiv:0810.3693].

[5] I. A. Shushpanov and A. V. Smilga, Phys. Lett. B **402**, 351 (1997).

[6] N. O. Agasian and I. A. Shushpanov, Phys. Lett. B **472**, 143 (2000).

[7] T.D. Cohen, D.A. McGady, E.S. Werbos, Phys. Rev. C **76**, 055201 (2007).

[8] S. P. Klevansky and R. H. Lemmer, Phys. Rev. D **39**, 3478 (1989); V.P.Gusynin, V.A.Miransky, I.A.Shovkovy, Nucl. Phys. B **462**, 249 (1996) [hep-ph/9509320]; D. Ebert, K. G. Klimenko, M. A. Vdovichenko and A. S. Vshivtsev, Phys. Rev. D **61**, 025005 (1999) [hep-ph/9905253].

[9] A. Goyal, M. Dahiya, Phys. Rev. D **62**, 025022 (2000) [hep-ph/9906367].

[10] A. V. Zayakin, JHEP **0807**, 116 (2008) [arXiv:0807.2917].

[11] P.V. Buividovich, M.N. Chernodub, E.V. Luschevskaya, M.I. Polikarpov, *"Numerical study of chiral symmetry breaking ..."*, arXiv:0812.1740.

[12] B. L. Ioffe and A. V. Smilga, Nucl. Phys. B **232**, 109 (1984).

[13] I. I. Balitsky, A. V. Yung, Phys. Lett. B **129**, 328 (1983); V. M. Belyaev, Y. I. Kogan, Yad. Fiz. **40**, 1035 (1984); I. I. Balitsky, A. V. Kolesnichenko, A. V. Yung, Sov. J. Nucl. Phys. **41**, 178 (1985); P. Ball, V. M. Braun, N. Kivel, Nucl. Phys. B **649**, 263 (2003) [arXiv:hep-ph/0207307].

[14] A. E. Dorokhov, Eur. Phys. J. C **42**, 309 (2005) [arXiv:hep-ph/0505007].

[15] A. E. Dorokhov, W. Broniowski and E. Ruiz Arriola, Phys. Rev. D **74**, 054023 (2006) [arXiv:hep-ph/0607171]; arXiv:0907.3374 [hep-ph].

[16] A. Vainshtein, Phys. Lett. B **569**, 187 (2003) [arXiv:hep-ph/0212231].

[17] A. Gorsky and A. Krikun, arXiv:0902.1832 [hep-ph].

[18] H. C. Kim, M. Musakhanov, M. Siddikov, Phys. Lett. B **608**, 95 (2005).

[19] V. M. Braun, S. Gottwald, D. Y. Ivanov, A. Schafer, L. Szymanowski, Phys. Rev. Lett. **89**, 172001 (2002); B. Pire, L. Szymanowski, Phys. Rev. Lett. **103**, 072002 (2009) [arXiv:0905.1258]; arXiv:0909.0098 [hep-ph].

[20] J. Rohrwild, JHEP **0709**, 073 (2007) [arXiv:0708.1405 [hep-ph]].

[21] T.D.Cohen, E.S.Werbos, Phys.Rev. C 80, 015203 (2009) [arXiv:0810.5103].

[22] P.V. Buividovich, M.N. Chernodub, E.V. Luschevskaya, M.I. Polikarpov, *"Chiral magnetization of non-Abelian vacuum ..."*, arXiv:0906.0488.

[23] D. Kharzeev, R.D. Pisarski, M. Tytgat, Phys. Rev. Lett. **81**, 512 (1998) [hep-ph/9804221]; D. Kharzeev, Phys. Lett. B **633**, 260 (2006).

[24] S. A. Voloshin, Phys. Rev. C **70**, 057901 (2004) [arXiv:hep-ph/0406311].

[25] S. A. Voloshin [STAR Collaboration], arXiv:0806.0029 [nucl-ex]; H. Caines [STAR Collaboration], arXiv:0906.0305 [nucl-ex].

[26] P.V. Buividovich, M.N. Chernodub, E.V. Luschevskaya, M.I. Polikarpov, *"CME in LGT"*, Pis'ma v ZhETF **90**, 456 (2009) and arXiv:0907.0494.

[27] P.V. Buividovich, M.N. Chernodub, E.V. Luschevskaya, M.I. Polikarpov, *"Quark electric dipole moment induced by magn. field"*, arXiv:0909.2350.

[28] V. G. Bornyakov et al, Phys. Rev. D **79**, 054505 (2009).

[29] H. Neuberger, Phys. Lett. B **417**, 141 (1998) [arXiv:hep-lat/9707022].

[30] M. H. Al-Hashimi and U. J. Wiese, Annals Phys. **324**, 343 (2009).

[31] P. H. Damgaard and U. M. Heller, Nucl. Phys. B **309**, 625 (1988).

[32] T. Banks and A. Casher, Nucl. Phys. B **169**, 103 (1980).

[33] S. J. Hands and M. Teper, Nucl. Phys. B **347**, 819 (1990).

[34] H. B. Nielsen and M. Ninomiya, Phys. Lett. B **130**, 389 (1983); M. A. Metlitski and A. R. Zhitnitsky, Phys. Rev. D **72**, 045011 (2005).